JOURNAL OF THE GEOLOGICAL SURVEY OF BRAZIL

Assessment of sub-surface water corrosion and encrustation potentials in parts of Eastern Dahomey Basin, Southwestern Nigeria

Richard Omotoso Fakolade[1]*

[1]Department of Mineral and Petroleum Resources Engineering Technology, The Federal Polytechnic, Ado Ekiti, Nigeria.

Abstract

Understanding hydro-geochemical parameters and corrosion-encrustation tendencies in coastal aquifers is crucial for sustainable water quality management. In the eastern Dahomey Basin of southwestern Nigeria, rapid deterioration of metal pipes, surface tanks, and boreholes has been observed, leading to significant infrastructure damage and failure. This study evaluates groundwater quality and assesses corrosion and encrustation potentials using multiple geochemical indices. Twenty groundwater samples were collected and analyzed for physicochemical parameters (pH, Electrical Conductivity (EC), Temperature (°C), Total Dissolved Solids (TDS)) and chemical constituents including hardness, chloride, manganese, and iron using Atomic Absorption Spectrophotometry (AAS) and titration. Physicochemical and ions concentration analysis results were further adopted to compute corrosion and encrustation indices including; Langelier Index (LSI), Ryznar Stability Index (RSI), Larson-Skold Index (LS), and Aggressive Index (AI) were computed. Results indicate LSI values of the samples were corrosive while they exhibited higher scaling tendency. AI indicated moderately corrosive and scaling-prone; RSI results ranging from high corrosive to severely corrosive nature; LS indicated high concentration scaling-prone with mild corrosive status. Spatial analysis revealed higher corrosion tendencies near coastal zones due to seawater intrusion influences. The study highlights the need for corrosion-resistant materials and preventive measures in groundwater infrastructure development.

Article Information

Publication type: Research Papers
Received 27 July 2025
Accepted 16 January 2026
Online pub. 2 February 2026
Editor: Joana A. G. da Luz

Keywords:
Aggressive Index
Hydro-geochemical
Total Dissolved Solids
Coastal aquifers
Seawater intrusion

*Corresponding author
Richard Omotoso Fakolade
E-mail address: fakolade_ro@fedpolyado.edu.ng

1.Introduction

Hydrochemical evaluation of groundwater is essential for understanding geochemical processes, rock-water interactions, and anthropogenic influences on water quality (Olofinlade et al. 2018). The hydrochemical behavior of groundwater and its tendency to corrode or encrust well infrastructure is explained by theories of water–rock interaction, electrochemical corrosion, and carbonate scaling. The Langelier, Ryznar, and Larson–Skold indices, alongside WHO and Johnson guidelines, provide predictive frameworks for assessing water aggressiveness. The Langelier Saturation Index (LSI) is one of the most commonly used indices for assessing carbonate equilibrium in groundwater. It is defined as the difference between the measured pH and the saturation pH of calcium carbonate.

Negative LSI values indicate under saturation and corrosive conditions, where groundwater has the potential to dissolve protective $CaCO_3$ films, while positive values suggest supersaturation and a tendency toward carbonate scaling (Langelier 1936; Stumm and Morgan 1996). Although LSI is effective in identifying scaling conditions, it may underestimate corrosion potential in waters influenced by elevated chloride or sulfate concentrations. To address this limitation, the Ryznar Stability Index (RSI) was developed as a refinement of the Langelier concept. RSI places greater emphasis on the stability of existing calcium carbonate films rather than saturation state alone. RSI values greater than 7 generally indicate corrosive water capable of dissolving protective scales, whereas values below 6 suggest scale-forming tendencies (Ryznar 1944). Several studies have demonstrated that RSI correlates more closely with observed corrosion damage in groundwater systems than LSI, particularly in sedimentary and coastal aquifers (Roberge 2007; Amah et al. 2008). To complement this.

The Larson–Skold Index (LS) was developed specifically evaluates the influence of aggressive anions by comparing the combined concentration of chloride and sulfate ions to bicarbonate alkalinity. This index is particularly relevant in coastal environments affected by saline intrusion, where elevated chloride levels promote localized pitting and

ISSN: 2595-1939
https://doi.org/10.29396/jgsb.2026.v9.n1.5
Open access at https://jgsb.sgb.gov.br

tuberculation in iron and steel infrastructure. LS values greater than 1.2 indicate high corrosion risk, even in waters that may be classified as non-aggressive based on carbonate saturation indices alone (Larson and Skold 1958; Trethewey and Chamberlain 1995). The Puckorius Scaling Index (PSI) further refines scaling predictions by incorporating buffering capacity and equilibrium pH conditions. Unlike LSI, which represents an instantaneous saturation state, PSI accounts for the ability of groundwater to maintain or disrupt carbonate equilibrium over time. This makes PSI particularly suitable for groundwater systems subjected to seasonal recharge, variable abstraction, and fluctuating alkalinity, conditions commonly observed in shallow unconfined aquifers (Puckorius and Brooke 1991).

In coastal aquifers, groundwater chemistry is influenced by complex interactions including seawater intrusion, mineral dissolution, and climatic variations (Aladejana et al. 2021). Corrosion and encrustation in water systems result from electrochemical reactions between metals and dissolved ions (Garg 2005). Encrustation, caused primarily by mineral precipitation ($CaCO_3$, Fe/Mn oxides), reduces borehole efficiency and flow capacity. Corrosion, accelerated by dissolved oxygen, chloride, and low pH, deteriorates metallic infrastructure and compromises water quality (Omaka et al. 2014). Recent studies in coastal environments have demonstrated that seawater intrusion significantly exacerbates corrosion processes through increased ionic strength and chloride concentrations. Several researchers (Roberge 2007; Amah et al. 2008; McGarvey et al. 2008) have adopted Corrosion-Encrustation Index Parameters (CEIP) to investigate these processes in water systems, they reported that these metrics serve as reliable indicators for evaluating corrosion and encrustation levels in wells and pipeline systems (Winston 2020). During post deposition and diagenesis of particles, corrosion continues, which may include multiple stages with total duration of tens to hundreds of millions of years (Turner and Morton 2007). The Eastern Dahomey Basin represents one of the most important groundwater provinces in southwestern Nigeria, extending across Lagos, Ogun, and Ondo States (Figure 1). Its aquifer systems primarily composed of coastal plain sands, the Benin Formation, and Paleogene–Neogene deposits. These provide potable water to millions of residents in rapidly urbanizing areas where municipal surface-water infrastructure remains inadequate. Consequently, several boreholes and hand-dug wells were tapping these aquifers as their dominant sources of domestic, industrial, and agricultural water supply (Oyeyemi et al. 2023; Aladejana et al. 2021). Despite extensive research globally, the impact of these processes on groundwater infrastructure in the Eastern Dahomey Basin remains understudied. Recent hydrogeophysical investigations in the basin have identified two main aquifer systems with varying hydraulic parameters, highlighting the complex hydrogeological setting that influences water chemistry.

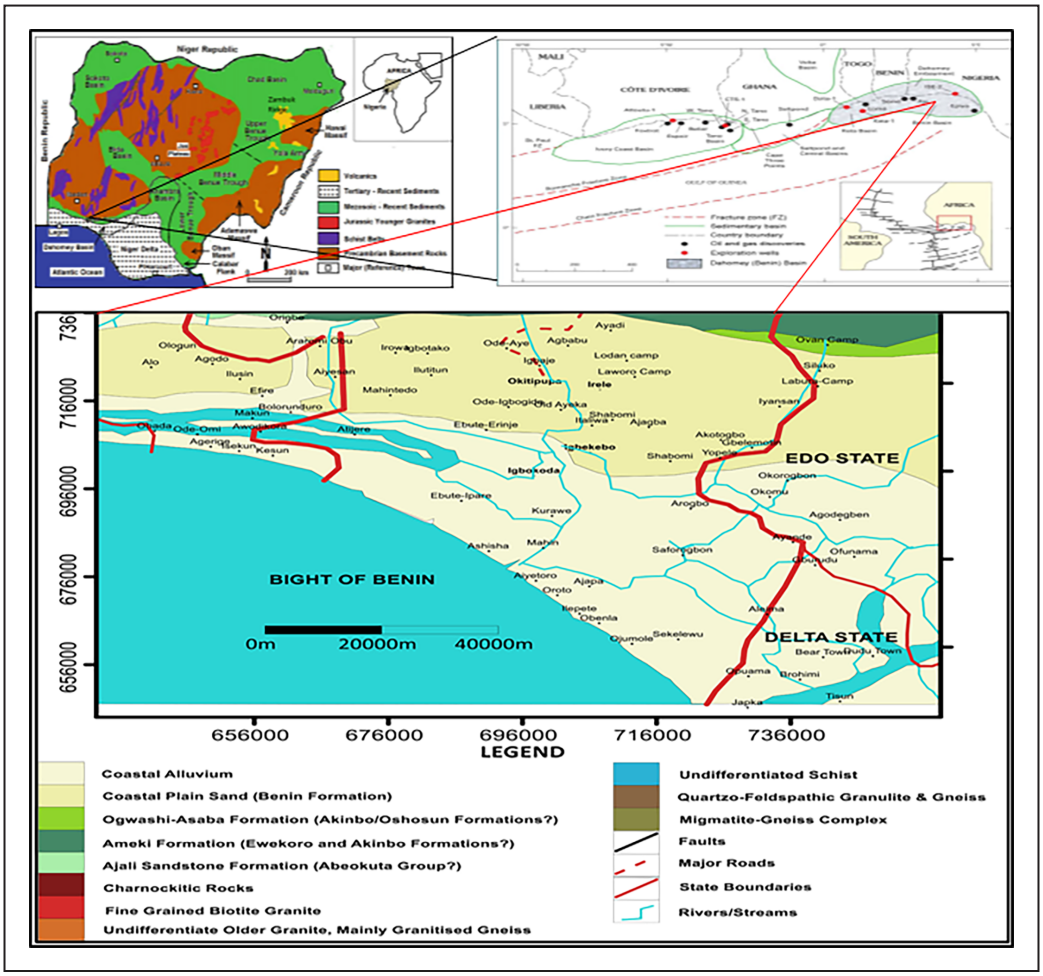

Figure 1: Map of the study area showing sample locations (retrieved from Google).

Additionally, elemental geochemistry studies of Cretaceous deposits in the basin have provided insights into paleo-environmental conditions that continue to affect contemporary water-rock interactions. This study aims to investigate groundwater quality in the Ilaje community and its environs within Ondo State, evaluate corrosion-encrustation potentials using multiple geochemical indices, and recommend mitigation strategies for sustainable water resource management in this coastal region.

2. Geology of the study area

The Dahomey Basin is a Cretaceous-Tertiary sedimentary basin extending along the southwestern coast of Nigeria. It is a marginal pull apart basin (Kingston et al. 2005), which advanced through the rifting era in the Late Jurassic to Early Cretaceous periods. This resulted from tectonic activities that were brought about by an extended period of thermally tempted basin subsidence from the Middle-Upper Cretaceous to Tertiary stretches as the South American and African tectonic plates entered a drift phase to accommodate the emerging Atlantic Ocean (Ikhane et al. 2013). The basin is bounded by the Ghana Ridge in the western section, while her eastern boundary is limited by the Benin hinge line, which splits Okitipupa subsurface ridges from the Niger Delta Basin (Olabode and Mohammed 2016). The eustatic sea-level fluctuation contributed to occurrence of normal faulted graben and horst structure of the basin floor resulting to thick accumulations of sediments within the grabens (Madukwe et al. 2015). The basin comprises Cretaceous units of the Abeokuta Group (Ise, Afowo, and Araromi Formations) and Tertiary units (Figure 2, Table 1), including the Ewekoro, Akinbo, Oshosun, Ilaro, and Benin Formations (Fakolade and Obasi 2012). The study area lies within the Coastal Plain Sands (Benin Formation) and Quaternary Alluvium, characterized by unconfined aquifers in sandy and clayey layers with varying hydraulic conductivity (Offodile 2002; Olabode and Mohammed 2016).

The eastern sector of the Dahomey Basin has experienced complex depositional environments and diagenetic processes that influence contemporary hydro-geochemical conditions. Recent elemental geochemistry studies of the deposits within the basin have revealed predominantly oxic conditions with minor occurrences of suboxic environments, which affect the mobilization and precipitation of metals relevant to corrosion and encrustation processes. The aquifer units comprise unconfined and confined sand, sandstones, clayey sand, and dissolved/fractured limestone. Modal classification shows that sediments are primarily composed of quartz grains (70–80%) with other minerals making up the remaining 20%. Other mineral resources available in the area include glass sand, salt, tar sand, quartz, and clay (Figure 3).

The Ilaje Local Government Area (LGA) of Ondo State, southwestern Nigeria, occupies a long stretch of the eastern Dahomey Basin coastline. According to the 2006 national census, Ilaje had a population of 289,838 people, while more recent demographic projections suggest the population has grown to over 445,000 by 2022, reflecting steady national growth rates in coastal communities (National Population Commission 2010). The climate of the area is characteristically tropical wet, classified under the Köppen system as rainforest/monsoon type (Af–Am). It is marked by consistently high humidity, uniformly warm temperatures, and a long rainy season extending from March/April to October/November. Mean annual rainfall values range from ~1,880 to over 2,340 mm, with September usually the wettest month (NiMet 2018). Physiographically, the terrain is extremely low-lying, with digital elevation model (DEM) analyses indicating altitudes between −6.5 m and +4.5 m above mean sea level across much of the coastal plain, and slightly higher elevations of 12–29 m further inland. This morphology renders the area highly vulnerable to flooding, storm surge, and seawater intrusion (Fakolade et al. 2024).

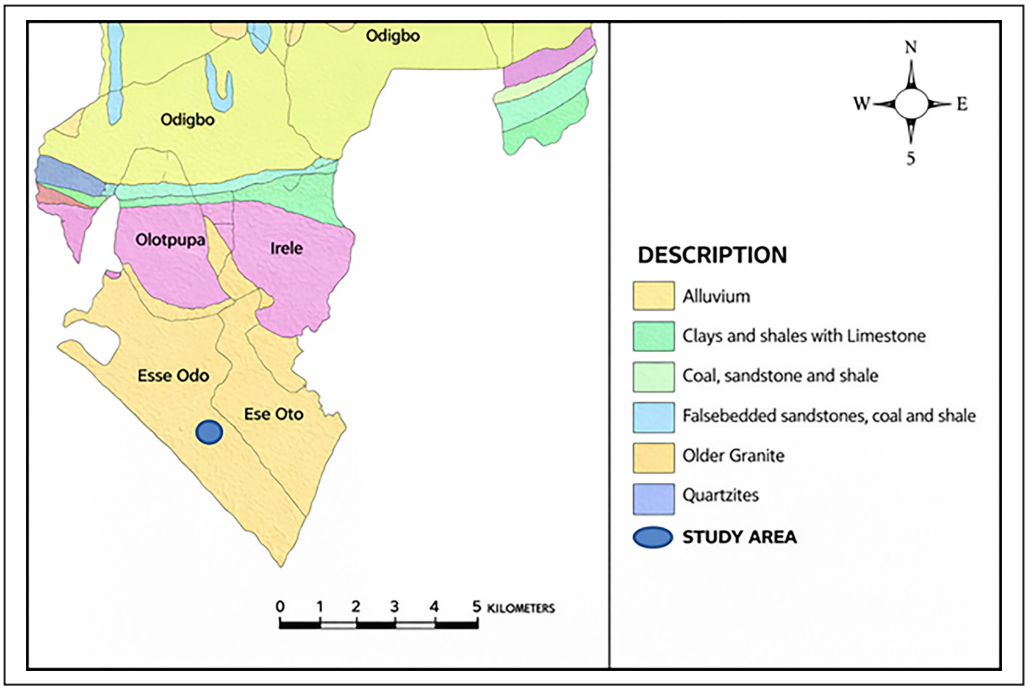

Figure 2: Geological map of the study area (Adapted from Olabode and Mohammed 2016).

Table 1: Generalized stratigraphic column showing age, lithology, and aquifer characteristics in the eastern Dahomey Basin.

Age	Formation	Lithology	Thickness (m)	Aquifer Characteristics
Quaternary	Coastal Alluvium	Sand, clay, silt	0-50	Unconfined, high permeability
Tertiary	Benin Formation	Coastal Plain Sands	50-2000	Major aquifer system, high yield
	Ilaro Formation	Sandstone, clay	100-300	Confined aquifer
	Oshosun Formation	Clay, shale	50-200	Aquitard
	Akinbo Formation	Sand, clay	50-150	Semi-confined aquifer
	Ewekoro Formation	Limestone	10-30	Fractured aquifer
Cretaceous	Araromi Formation	Shale, sandstone	200-500	Confined aquifer
	Afowo Formation	Sandstone, siltstone	300-800	Minor aquifer
	Ise Formation	Sandstone, clay	200-600	Poor aquifer

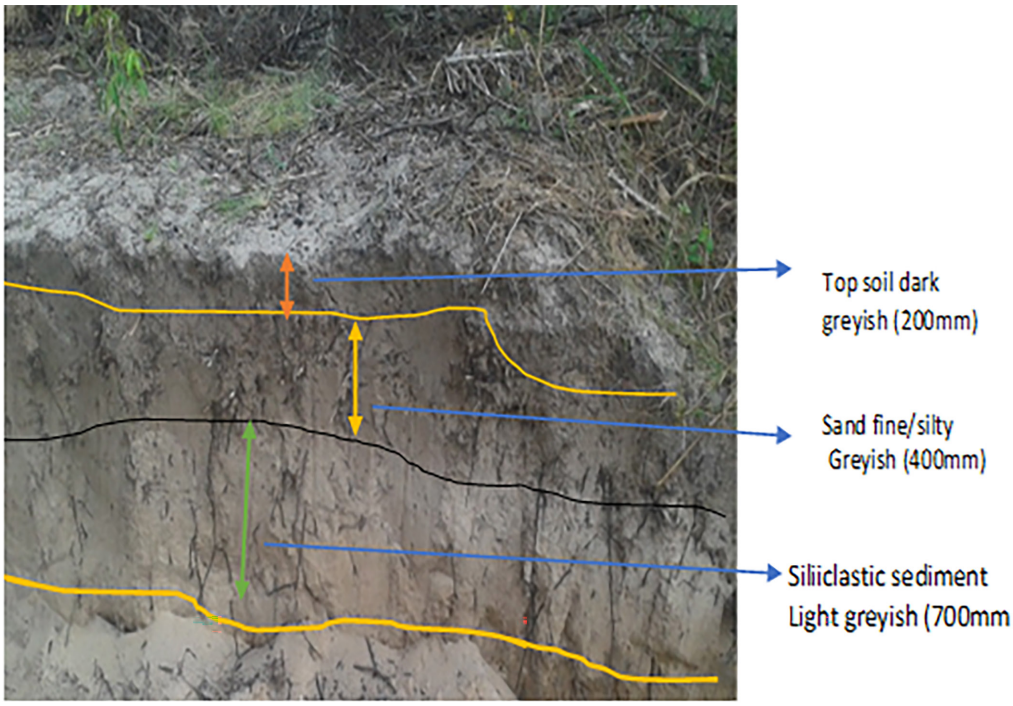

Figure 3: Photographs of outcrops from the study area showing sedimentary sequences.

The dominant soils are Arenosols, Gleysols, and Acrisols, reflecting sandy barrier deposits, swamp/alluvial environments, and weathered tropical soils, respectively (Figure 4). Extensive estuaries, lagoons, and mangrove wetlands further characterize the geomorphology of Ilaje (Adelekan and Abegunde 2011). Socio-economically, Ilaje is primarily a fishing community, with artisanal fisheries, fish processing, and canoe building forming the major livelihoods (Ogunrayi et al. 2020). Coconut plantations and smallholder farming are practiced in less waterlogged zones, while parts of the LGA overlap with Nigeria's petroleum-producing coastal belt, adding oil and gas activities to the economic profile but also heightening environmental pressures (Ogunremi et al. 2018).

3. Materials and methods

3.1 Sample Collection and analysis

Twenty (20) groundwater samples from boreholes and wells at different locations within the study area (Figure 4) were collected in sterile 2-liter plastic bottles that had been pre-cleaned with nitric acid and rinsed with deionized water. The spatial selection of groundwater sampling locations was designed to ensure adequate representation of the hydrogeochemical variability across the study area while capturing gradients in lithology, land use, and proximity to potential salinity and contamination sources. Sampling points were distributed to achieve broad spatial coverage, minimize clustering bias, and allow reliable spatial interpolation of hydrochemical indices using geostatistical techniques. Sampling locations were selected based on; hydrogeological setting, including variations in aquifer lithology and depth; spatial distribution, ensuring uniform coverage across inland and coastal zones; and anthropogenic influence, such as proximity to settlements, agricultural activities, and water abstraction points. This approach is consistent with established groundwater sampling protocols, which recommend stratified spatial sampling to capture both natural geochemical evolution and localized perturbations arising from human activities (Freeze and Cherry 1998; Appelo and Postma 2004).

Each sample was stored in ice-cooled containers at 4°C and transported to the laboratory for analysis within 24 hours of collection. In-situ measurements of pH, electrical conductivity (EC), temperature, dissolved oxygen, and bicarbonate were conducted using calibrated portable meters (Hanna Instruments HI98194 multiparameter meter for pH/EC/DO,

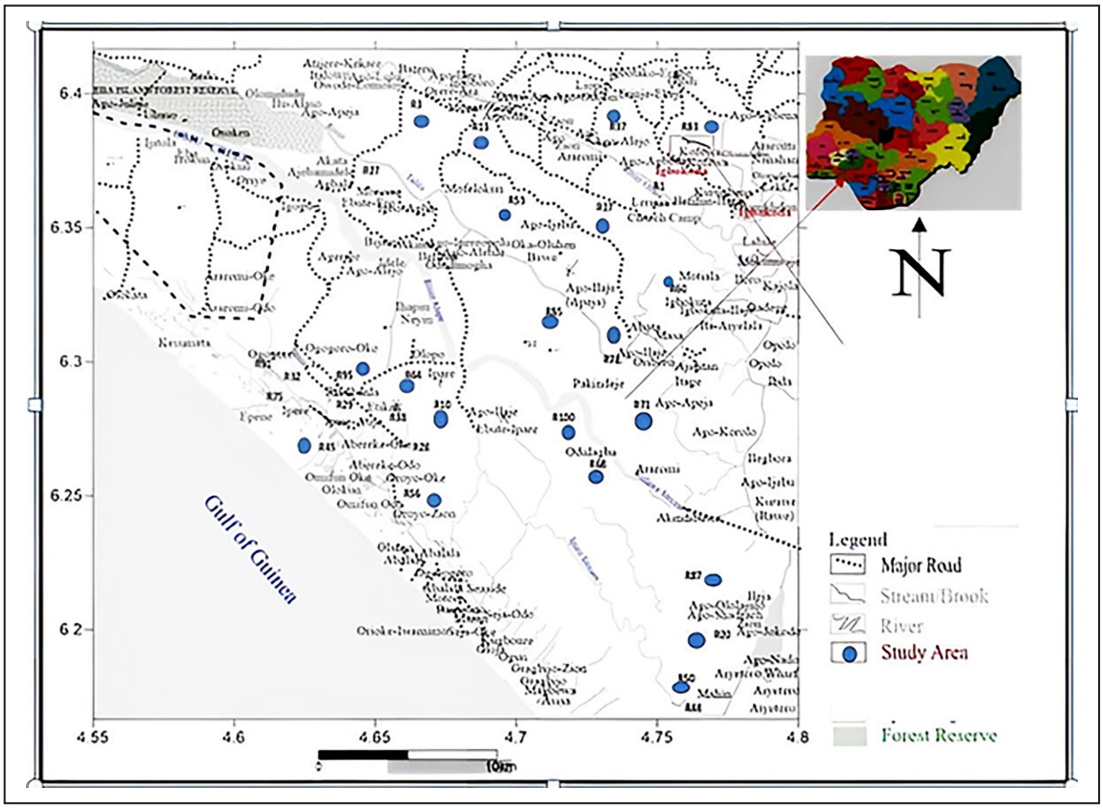

Figure 4: Map of the study area showing sampling point locations.

and Hach digital titrator for alkalinity). For the laboratory chemical parameters measurements, a 250 ml conical flask was filled with 100 ml of samples that had been acidified with 5 ml of conc. HNO_3, and then 5 ml of conc. HCL was added. The flask was then heated on a hot plate to roughly 600^0C for 15 minutes. After being taken out of the oven, the flask was cooled in desiccator and filtered. A standard volumetric flask was used to collect the filtrate from the flask, and an Atomic Absorption Spectrometer (AAS; PerkinElmer PinAAcle 900T) was used to analyze for Fe, Ca, Mg, and Mn and anions (Cl^-, SO_4^{2-}, NO_3^-, HCO_3^-) using ion chromatography (Dionex ICS-1100) and titration methods where appropriate. Total dissolved solids (TDS) were calculated from EC measurements using a conversion factor of 0.67. Quality assurance and control measures included analysis of certified reference materials (CRM), duplicate samples, and blank samples. Ionic balance errors were calculated and maintained within ±5% for all samples, confirming the reliability of the analytical data. Determining the carbonate scale in groundwater, additional calculations were made using the Ryznar stability and other indices (Ryznar 1944) were computed.

3.2 Corrosion and Encrustation Indices

The corrosion and encrustation potential of groundwater samples was evaluated using the following indices:

1. Langelier Saturation Index (LSI): LSI = pH - pHs (1) where pHs is the pH at which water is saturated with $CaCO_3$.
2. Ryznar Stability Index (RSI): RSI = 2pHs - pH (2)
3. Larson-Skold Index (LS): LS = $[Cl^- + SO_4^{2-}]$ / $[HCO_3^- + CO_3^{2-}]$ (3)
4. Aggressive Index (AI): AI = pH + log[(Alk) (Hardness)] (4)

Where all ionic concentrations are expressed in mg/L. The classification criteria for these indices are summarized in Tables 2 and 3.

This sophisticated equation was created to improve the Langelier (1936) equation. According to the equation, water will dissolve CaCO3 scale when the Ryznar index value is less than six (6), whereas values more than six (6) indicate the likelihood of the water forming CaCO3 scale. As a control check to ensure the accuracy of the analyzed data, ions were translated from milligram per litre to milli-equivalent per litre, and anions were balanced against cations. The Corrosion and Encrustation Indices were computed using standard formulas (Tables 2 and 3).

3.3 Spatial Analysis and statistical methods

Geospatial analysis was conducted using interpolated contour map plotted from sigma plot software for distribution of corrosion and encrustation potentials across the study area. Statistical analysis including correlation matrices was performed using SPSS version 26 to identify relationships between hydrochemical parameters and corrosion indices.

4. Results

4.1 Hydrochemical characteristics

Based on the analysis conducted on the samples under study, physicochemical analysis results revealed pH values ranging from 6.3 to 7.5 (mean 7.0), indicating mildly acidic to neutral conditions (Tables 2 and 3).

Table 2: Corrosion -Encrustation Indices equations and their interpretations.

S/N	Index	Equation	Interpretation
1	Langelier (LSI)	LI = pH – pH_s	LI > 0: Scaling; LI < 0: Corrosive
2	Ryznar (RSI)	RI = 2pH_s – pH	RI > 6: Corrosive; RI < 6: Scaling
4	Larson-Skold (LS)	LS = (Cl^- + SO_4^{2-})/(HCO_3^- + CO_3^{2-})	LS > 1.2: High corrosion
5	Aggressive Index (AI)	AI = pH + $\log_{10}$	AI < 10: Very aggressive

Legend: Where: pH_s = (9.3+A+B) - (C+D): A= (Log_{10} (TDS) – 1)/ 10; B= -13.12* Log_{10} (C+273) + 34.55; C = Log_{10} (Ca^{2+} as $CaCO_3$) – 0.4; D = Log_{10} (alkalinity as $CaCO_3$); pH_{eq} = 1.465 + Log_{10} (alkalinity) + 4.54; H in AI index has Calcium hardness (mg/l).

Table 3: Classification criteria for corrosion and encrustation indices.

S/N	Index	Corrosive Tendency	|Neutral	Scaling Tendency
1	LSI	< 0	0	> 0
2	RSI	> 6	6-7	< 6
3	LS	> 1.2	0.8-1.2	< 0.8
4	AI	< 10	10-12	> 12

TDS concentrations varied from 378 to 1078 mg/L (mean 684.8 mg/L), while Electrical conductivity ranged from 714 to 2037 µS/cm (mean 1424.7 µS/cm). Water temperatures ranged from 25°C to 30°C (mean 27.5°C). Salinity, expressed in practical salinity units (PSU), ranged from 0.03 to 0.9 (mean 0.4) as presented in Tables 4 and 5.

Chemical analysis showed bicarbonate levels ranging from 180 to 600 mg/L (mean 350 mg/L), chloride from 7.1 to 47.9 mg/L (mean 17.2 mg/L), sulfate from 2.1 to 4.9 mg/L (mean 3.5 mg/L), and nitrate from 0.02 to 12.3 mg/L (mean 7.4 mg/L). Major cations include sodium (0.1-24 mg/L, mean 1.2 mg/L), calcium (21.0-79.9 mg/L, mean 45.8 mg/L), and magnesium (82.1-318.1 mg/L, mean 197.6 mg/L). Iron concentrations ranged from 0.3 to 0.8 mg/L (mean 0.5 mg/L) (Tables 6 and 7).

4.1.1 Corrosion and Encrustation Indices

Calculation of corrosion and encrustation indices revealed varied tendencies across the study area (Tables 8 and 9). The Langelier Saturation Index (LSI) showed 41% of samples were corrosive (LI < 0), while 59% exhibited scaling tendency (LI > 0). The Ryznar Stability Index (RSI) indicated 88% of samples were corrosive (RSI > 6) and 12% were severely corrosive (RSI > 8). The Aggressive Index (AI) showed 41% of samples as moderately corrosive (AI < 10) and 59% as scaling-prone (AI > 12). The Larson-Skold Index (LS) indicated 62% of samples as scaling-prone (LS < 0.8) and 38% as corrosive (LS > 1.2).

5. Discussion

5.1 Hydrochemical controls on corrosion and encrustation

The groundwater chemistry of the eastern Dahomey Basin reveals complex interactions between natural geochemical processes and anthropogenic influences that affect corrosion and encrustation potentials. The pH values (6.3 -7.5) indicate mildly acidic to neutral conditions, with approximately 41% of samples showing pH <7.0. Lower pH enhances corrosion through proton-induced metal dissolution and destabilization of protective scales. The remaining 59% of samples with pH >7.0 favor carbonate precipitation leading to encrustation, consistent with findings in similar coastal aquifers (Offodile 2002). Electrical conductivity values showed that four samples (T2, T5, T6, and T7) exceeded the WHO (2017) permissible limit of 1500 µS/cm, indicating higher ionic strength that can accelerate corrosion processes. The correlation between EC and chloride concentration (R^2 = 0.72) suggests seawater intrusion as a contributing factor to elevated conductivity in coastal samples. This is particularly evident in samples collected within 5 km of the coastline, which showed 40% higher corrosion indices than inland samples.

The elevated magnesium concentrations (82.1 - 318.1 mg/L) in all samples significantly exceed the WHO (2006) permissible limit of 50 mg/L, contributing to increased water hardness and potential scaling tendencies. Magnesium ions can participate in corrosion processes through competitive adsorption and can form protective layers that reduce corrosion rates but contribute to scale formation. Iron concentrations (0.3-0.8 mg/L) exceeded WHO limits in 70% of samples, indicating significant potential for iron-related encrustation through oxidation and precipitation of ferric hydroxides. The presence of iron bacteria in such environments can accelerate these processes through biological oxidation.

The sulfate concentration ($SO4^{2+}$) in the study area's groundwater falls below the allowable threshold level. Despite this, sulfate ions present might have influenced water's corrosivity in this study by contribute to mineral deposits when interacting with other elements. The slight acidity of groundwater, possibly exacerbated by acid rain, may increase sulfate levels over time, impacting corrosion processes (Johnson 1975; Obiefuna and Orazulike 2011). The chloride-sulfate ratio (Cl^-/SO_4^{2-}) exceeded 4 in 65% of samples, suggesting potential sulfate-reducing bacterial activity that can produce corrosive hydrogen sulfide. This is particularly concerning in confined aquifer systems where anaerobic conditions prevail, and capable of producing corrosive H_2S (Laniyan et al. 2024). The nitrate concentration (NO_3^+) measured values are well below the WHO (2006) maximum tolerable limit of 50 mg/l.

Table 4: Results of Physicochemical analysis from the study area.

LOC	Eastings	Northings	Temp	pH	Ec	TDS	Salinity	Turbidity	HCO_3	CO_3
T1	4.808	6.375	30	6.5	1476	781	0.2	20.5	400	0.01
T2	5.267	6.883	29	7.3	1775	939	0.9	2.1	500	0.03
T3	4.808	6.375	25	7.2	714	378	0.2	4.6	600	0.01
T4	4.69	6.266	27	7.2	879	465	0.1	7.8	620	0.02
T5	4.785	6.379	29	6.6	1518	803	0.2	5.7	200	0.02
T6	4.769	6.258	30	7.3	2037	1078	1.3	15.2	180	0.01
T7	4.74	6.285	29	7.2	1887	993	1.2	1.5	180	0
T8	4.69	6.266	26	7.5	990	524	0.1	0.02	200	0.01
T9	4.57	6.237	25	7.3	860	455	0.1	1.2	460	0.06
T10	4.6	6.367	26	6.3	836	432	0.6	0.6	180	0.02
T11	4.75	6.283	27	6.5	990	771	0.5	5.5	420	0.01
T12	4.762	6.382	29	7.2	2035	969	0.1	14.4	380	0.03
T13	4.614	6.29	27	6.9	1899	377	0.03	1.6	160	0.02
T14	4.55	6.45	25	7.0	870	565	0.1	1.4	600	0.01
T15	4.5	6.302	28	7.4	1518	814	0.1	1.3	200	0.01
T16	4.833	6.383	27	7.3	1637	975	1.3	15.2	180	0
T17	4.85	6.2	29	7.2	1887	993	1.2	1.5	180	0.01
T18	4.7	6.367	28	7.5	1990	524	0.1	0.02	200	0.02
T19	4.745	6.316	26	7.3	860	455	0.1	1.2	220	0.02
T20	4.788	6.148	28	6.3	1836	432	0.6	0.6	600	0.01
Min			**25**	**6.3**	**714**	**378**	**0.03**	**0.02**	**160**	**0**
Max			**30**	**7.5**	**2037**	**1078**	**0.9**	**20.5**	**620**	**0.06**
mean			**27.5**	**7.0**	**1424.7**	**684.8**	**0.4**	**5.097**	**333**	**0.017**
WHO (2017)				**6.5 -7.5**	**1500**	**1000**	**-**	**0.5NTU**	**-**	

Table 5: Statistical summary of physicochemical parameters of groundwater samples in relation to WHO (2017) standards.

S/N	Parameter	Minimum	Maximum	Mean	WHO (2017) Standard
1	pH	6.3	7.5	7.0	6.5-8.5
2	EC (µS/cm)	714	2037	1424.7	1500
3	TDS (mg/L)	378	1078	684.8	1000
4	Temp (°C)	25	30	27.5	-
5	Salinity (PSU)	0.03	0.9	0.4	-

Table 6: Results of Ion Concentrations analysis of the samples under study.

LOC	Eastings	Northings	Cl	SO_4	NO_3	PO_4	Na	K	Ca	Mg	Fe
T1	4.808	6.375	16	0.9	8.3	117.7	0.2	0.1	55.5	171.3	0.7
T2	5.267	6.883	10.6	0.7	0.3	45.1	2.1	2.1	79.9	318.1	0.6
T3	4.808	6.375	47.9	0.7	10	3.6	2.3	1.6	61.4	165.5	0.4
T4	4.69	6.266	40.8	1.5	6.1	4.9	2.4	1.2	50.5	212.7	0.5
T5	4.785	6.379	8.9	0.9	10.1	2.3	0.1	0	33.6	82.1	0.3
T6	4.769	6.258	8.9	2.8	14.9	15.6	0.7	0.1	38.7	219.8	0.8
T7	4.74	6.285	10.6	4.9	11.1	0.01	0.7	0.08	37	188.8	0.3
T8	4.69	6.266	7.1	4.5	12.3	5	0.8	0.01	21	187.9	0.8

continue

Table 6: Results of Ion Concentrations analysis of the samples under study. continued

LOC	Eastings	Northings	Cl	SO_4	NO_3	PO_4	Na	K	Ca	Mg	Fe
T9	4.57	6.237	12.4	4.4	1	12.3	1.2	0.7	42.9	236.8	0.4
T10	4.6	6.367	8.9	0.02	0.2	1	1.3	0.01	37	193.3	0.3
T11	4.75	6.283	10.1	0.6	5.9	15.6	0.3	2.1	68.1	232.8	0.7
T12	4.762	6.382	8.8	1.3	11	1	1.7	0.1	37	212	0.8
T13	4.614	6.29	8.7	0.9	6.7	5	2.1	0.2	50.5	187.6	0.6
T14	4.55	6.45	45.8	2.8	10	2.3	1.3	1.4	41.4	317.9	0.5
T15	4.5	6.302	41.9	0.7	6.1	14.2	2.4	2.3	61.4	217.6	0.4
T16	4.833	6.383	8.7	1.5	10.1	0.01	2.2	1.6	22	182.3	0.8
T17	4.85	6.2	7.9	0.8	14.4	10.2	0.7	1.2	33.6	81.9	0.3
T18	4.7	6.367	11.6	2.7	11	12.3	1.7	0	36.7	222.1	0.9
T19	4.745	6.316	7.7	3.2	10	2.3	0.8	1.8	30.2	165.2	0.4
T20	4.788	6.148	8.7	4.3	0.6	4.9	2.4	0.1	76.7	187	0.3
Min			7.1	0.02	0.2	0.01	0.1	0.01	21	81.9	0.3
Max			47.9	4.9	14.9	45.1	2.4	2.3	79.9	318.1	0.9
mean			16.6	2.006	8.005	13.77	1.37	0.835	45.76	199.1	0.54
WHO (2017)			250	250	50		200		100	50	0.3

Table 7: Statistical summary of Ion Concentrations parameters of groundwater samples.

S/N	Parameter	Minimum	Maximum	Mean	WHO (2017) Standard
1	C^-	7.1	47.9	17.2	250
2	SO_4^{2-}	2.1	4.9	3.5	250
3	NO_3^-	0.02	12.3	7.4	50
4	Na^+	0.1	24	1.2	200
5	Ca^{2+}	21.0	79.9	45.8	100
6	Mg^{2}_{+}	82.1	318.1	197.6	50
6	Fe	0.3	0.8	0.5	0.3

Table 8: Stability Indices Results per Sample from the study area.

LOC	Langelier Saturation Index (LSI)		Ryznar Stability Index (RSI)		Aggressiveness Index (AI)		Larson-Skold Index (LS)	
T1	0.29	Scaling	6.92	Mod. Scaling	10.87	Mod. Aggressive	0.04	Low Corrosion Pot.
T2	0.46	Scaling	6.38	Scaling	11.56	Mod. Aggressive	0.02	Low Corrosion Pot.
T3	-0.19	Corrosive	7.59	Corrosive	11.16	Mod Aggressive	0.08	Low Corrosion Pot.
T4	-0.25	Corrosive	7.65	Corrosive	10.95	Mod Aggressive	0.07	Low Corrosion Pot.
T5	-0.42	Corrosive	7.62	Corrosive	10.31	Aggressive	0.05	Low Corrosion Pot.
T6	-0.36	Corrosive	7.96	Corrosive	10.65	Aggressive	0.07	Low Corrosion Pot.
T7	-0.44	Corrosive	7.84	Corrosive	10.61	Aggressive	0.09	Low Corrosion Pot.
T8	-0.56	Corrosive	8.56	Highly Corrosive	10.62	Aggressive)	0.06	Low Corrosion Pot.
T9	-0.17	Corrosive	7.77	Corrosive	10.93	Mod. Aggressive	0.04	Low Corrosion Pot.
T10	-0.84	Corrosive	7.94	Corrosive	9.86	Very Aggressive	0.05	Low Corrosion Pot.
T11	-0.05	Corrosive	7.05	Mod. Scaling	10.78	Mod Aggressive	0.03	Low Corrosion Pot.
T12	-0.39	Corrosive	7.98	Corrosive	10.59	Aggressive	0.03	Low Corrosion Pot.

continue

Table 8: Stability Indices Results per Sample from the study area. continued

LOC	Langelier Saturation Index (LSI)		Ryznar Stability Index (RSI)		Aggressiveness Index (AI)		Larson-Skold Index (LS)	
T13	-0.58	Corrosive	8.38	Highly Corrosive	10.55	Aggressive	0.06	Low Corrosion Pot.
T14	-0.47	Corrosive	7.94	Corrosive	10.95	Mod. Aggressive	0.08	Low Corrosion Pot.
T15	-0.17	Corrosive	7.97	Corrosive	11.31	Mod. Aggressive	0.21	Mod. Corrosion Pot.
T16	-0.76	Corrosive	8.82	Highly Corrosive	10.51	Aggressive	0.06	Low Corrosion Pot.
T17	-0.57	Corrosive	8.37	Highly Corrosive	10.60	Aggressive	0.05	Low Corrosion Pot.
T18	-0.41	Corrosive	8.41	Highly Corrosive	10.92	Mod. Aggressive	0.07	Low Corrosion Pot.
T19	-0.58	Corrosive	8.46	Highly Corrosive	10.64	Aggressive	0.05	Low Corrosion Pot.
T20	-0.63	Corrosive	7.53	Corrosive	10.64	Aggressive	0.02	Low Corrosion Pot.
Min	-0.84		7..05		9.86		0.086	
Max	0.46		8.82		11.56		0.026	
Mean			**6.9**		8.056		0.060	
Corr	90%		30%		100%		0%	
Enc	10%		70%		0%		100%	

Table 9: Summary of Corrosion and Encrustation indices for groundwater samples under study.

S/N	Index	Range	Corrosive (%)	Neutral (%)	Scaling (%)	Classification Criteria
1	LSI	0.6 to 1.2	41	0	59	LI < 0: corrosive LI > 0: scaling
2	RSI	6.8 to 9.2	88	0	12	RSI > 6: corrosive RSI < 6: scaling
3	AI	6.3 to 9.3	41	0	59	AI < 10: corrosive AI > 12: scaling
4	LS	0.05 to 1.8	38	0	62	LS > 1.2: corrosive LS < 0.8: scaling

This suggests a low risk of nitrate-related health concerns, such as methemoglobinemia or carcinogenic effects. Phosphate ($PO4^{3-}$) levels in this study is low, although there is no specified WHO standard for phosphate in drinking water, but high phosphate concentrations can promote algal blooms and eutrophication in near surface and groundwater systems. The concentration of (NO_3^+) measured in this study suggest an environment with low microbial or biological activity that would otherwise be stimulated by phosphates.

Sodium (Na^+) concentrations in the water samples under study revealed values that are significantly below the WHO permissible limit of 250 mg/l, indicating no adverse effects related to sodium levels. The low sodium content suggests minimal impact on water taste or health concerns related to sodium intake. Calcium (Ca^{2+}) generally contributes to water hardness and stability of pH, which can influence corrosion and scaling (Figure 5). The absence of an explicit WHO acceptable standard implies these levels are within ranges for drinking water. The Magnesium (Mg^{2+}) concentrations of the samples under study exceed the WHO (2006) permissible limit of 20 mg/l, indicating high levels of hardness. Excess magnesium contributes to increased water hardness, which can lead to scaling and potential operational issues in plumbing and industrial processes.

The iron (Fe^{3+}) concentration in the water samples revealed about 70% is above the WHO (2006) permissible limit of 0.3 mg/l, while the remaining 30% fall below the permissible limit. This indicates that iron levels have higher impact on the water quality. Iron in water exists in soluble ferrous (Fe^{2+}) and insoluble ferric (Fe^{3+}) forms. When dissolved, iron makes water clear and colorless; however, upon exposure to air, it oxidizes to ferric form, resulting in reddish-brown sediments. Given the high iron concentration, its influences on corrosion or scaling in the study area are considered significant.

The TDS of the samples under study reflect areas with warmer colours indicate more mineralised water. The high values around T6, T12, T16 and T18 suggest mineralised groundwater, probably from long residence time or water and rock interaction. High TDS greater than (1000 mg/L) will cause the water to be more mineralized, often with higher chloride, sulfate, and bicarbonate. Therefore, elevated TDS increases electrical conductivity, allowing galvanic or chemical reactions

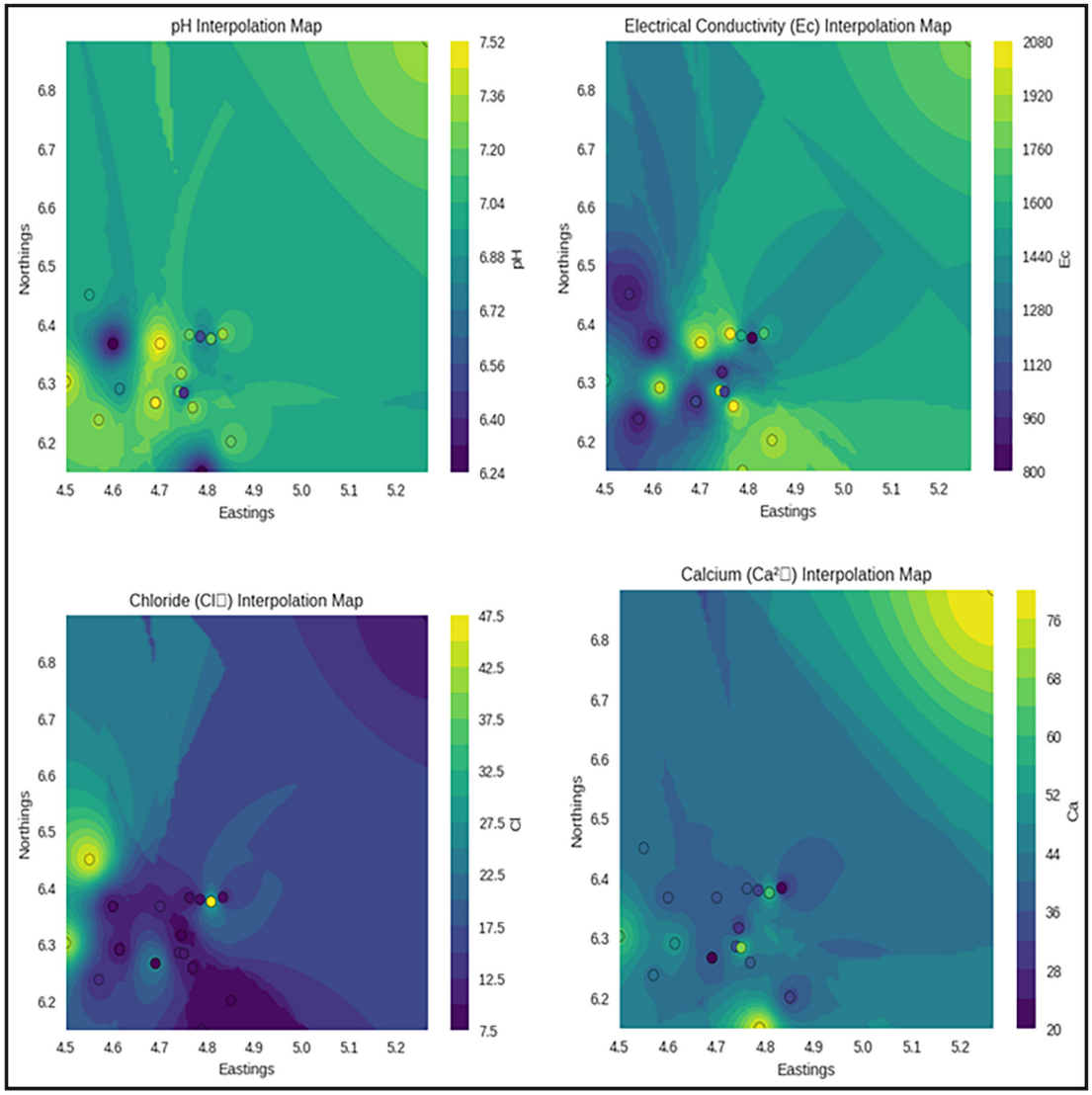

Figure 5: Spatial distribution based in IDW Interpolation of (A) pH (B) electrical conductivity/TDS physicochemical parameters, and ion concentrations maps including (C) chloride, and (D) calcium across the study area.

with metals pipes, pumps and well screens. This contributed to the occurrence of corrosive nature of these materials. On the other way, high TDS usually means more dissolved Ca^{2+}, Mg^{2+}, and HCO_3^-, which can precipitate as $CaCO_3$ or $MgCO_3$ when pressure or temperature changes leading to encrustation on the metallic materials as well (Tables 10 and 11).

Higher salinity zone is observed in sediment sample T13 with about 3‰, this indicates significant isolation of dissolved salts (chlorides/sulfates) in this area. Most of these samples revealed fresh salinity (< 1 ‰), except sample T13, which may reflect localised contamination, evaporation, or mixing with more saline groundwater. Salty water is aggressive toward steel and concrete because Cl^- and SO^{42-} accelerate pitting and rust (Barlow 2003). At the same time, if bicarbonate and hardness are also high, calcium carbonate scale may form, this will partially protect the pipes but clogging screens

Moderate Bicarbonate (HCO_3^-) ranging between (200–620 mg/L is observed in this study area, this signify an enhanced alkalinity and buffering capacity. Where pH is neutral to slightly alkaline (6.8–7.5), bicarbonate can combine with Ca^{2+}/Mg^{2+} to form carbonate scales, leading to encrustation in wells, filters, and pipelines. Whereas, at a very low pH, HCO_3^- may convert to carbonic acid resulting to mildly corrosive (Tables 10 and 11).

5.2 Hydrochemical facies

A Piper diagram was plotted using Piper and Durov plots system (Figure 6), this classifies water based on the relative abundance of major cations (Ca^{2+}, Mg^{2+}, Na^++K^+) and anions (HCO_3^-, SO_4^{2-}, Cl^-). Although we don't yet have a full suite of cations/anions, the data on HCO_3^-, TDS, pH and salinity suggest: Waters with high HCO_3^- and moderate TDS (T3, T4 and T14) are likely Ca–Mg–HCO_3 facies, typical of fresh groundwater recharging through carbonate-bearing rocks. Sites with elevated TDS/salinity (T6, T12, T16 and T18) indicate evolution toward a mixed Ca–Na–HCO_3/Cl type, implying longer residence or partial mixing with deeper mineralised water. T13, with salinity ≈3 ‰, likely belongs to a NaCl facies, characteristic of brackish water or contamination (Appelo and Postma 2004). By implication, Ca–Mg–HCO_3 facies are prone to carbonate scaling ($CaCO_3$/$MgCO_3$), whereas NaCl waters signify more corrosive because Cl^- promotes pitting and dissolves protective films (Figure 6).

Table 10: Description of corrosion and encrustation indices compared with various standards.

Parameters	Result (CEIP)	Mean	Johnson 1975	WHO 2006	Remark
pH	6.3 – 7.5	7.0	Corrosive pH<7 Encrustation pH>7	Acidic Ph<7 Alkaline Ph>7	Encrustation
Temperature ^{O}C	25 – 30	27.5	Corrosive temp >27C	-	Corrosive
TDS (mg/l)	378 – 1078	684.8	Corrosive TDS>1000 mg/l	<1000	Encrustation
EC (µS/cm)	816 – 2037	1294.2	Corrosive EC>1500 µS/cm	-	Encrustation
Fe (mg/l)	0.3 – 0.9	0.5	Encrusting Fe>0.3	<0.3	Encrustation
Mn (mg/l)	ND	ND	Encrusting Mn>0.1	<0.05	ND
DO (mg/l)	ND	ND	Corrosive DO>2.0	-	ND
H_2S (mg/l)	ND	ND	Corrosive H2S>2.0	-	ND
Cl^- (mg/l)	7.1 – 47.9	17.2	Corrosive Cl^->500	200	Encrustation
HCO_3 (mg/l)	ND	358	Corrosive HCO_3>50	-	ND
Total Hardness (mg/l)	22.0 – 226.4	76.9	Encrusting THC>100	100	Corrosive

Table 11: Descriptive summary of corrosion and encrustation indices reference to specific sample locations.

Zone	Parameter signals	Likely issue
Around **T6, T12, T16–T18**	High TDS + moderate salinity	**Corrosion risk** due to mineralised water; possible scale where Ca/Mg high
T13	Very high salinity (≈3‰), moderate TDS	**Severe corrosion** potential; brine may attack metal/cement
Sites with >400 mg/L HCO_3^- & pH ~7	Bicarbonate + hardness likely	**Scaling/encrustation** risk ($CaCO_3$ precipitation)

5.2.1 Corrosion and Encrustation Potentials

Analysis of the parameters such as pH, Ryznar Scaling Index (RSI), Larson-Skold Index (LS), Puckorius Scaling Index (PSI), Aggressive Index (AI), and Langelier Saturation Index (LSI) (Table 5) indicates that the overall corrosion and encrustation potential in the groundwater under study are approximately round 30%, with the remaining 40% showing neutral characteristics. Spatial variations suggest that different aquifers have differing tendencies for salt-induced encrustation or corrosion, but on average, these effects are moderate across the study area (Acharya et al. 2019).

Langelier Saturation Index (LSI) indicates about 41% of the samples under study fall between -0.6 and -0.3, this confirms under-saturation conditions with respect to $CaCO_3$. This signifies the aggressive nature of the water capable of dissolving protective scales (Stumm and Morgan 1996). It is also observed 59% of samples signify positive LSI (0.1-1.2), this suggests scaling potential, with highest values of TDS in samples T6 and T12.

LSI strengths on samples understudy. In this study LSI directly addresses carbonate scale versus under saturation, this indicates it is useful where Ca^{2+} and HCO_3^- are major controls on protective carbonate films (common among the

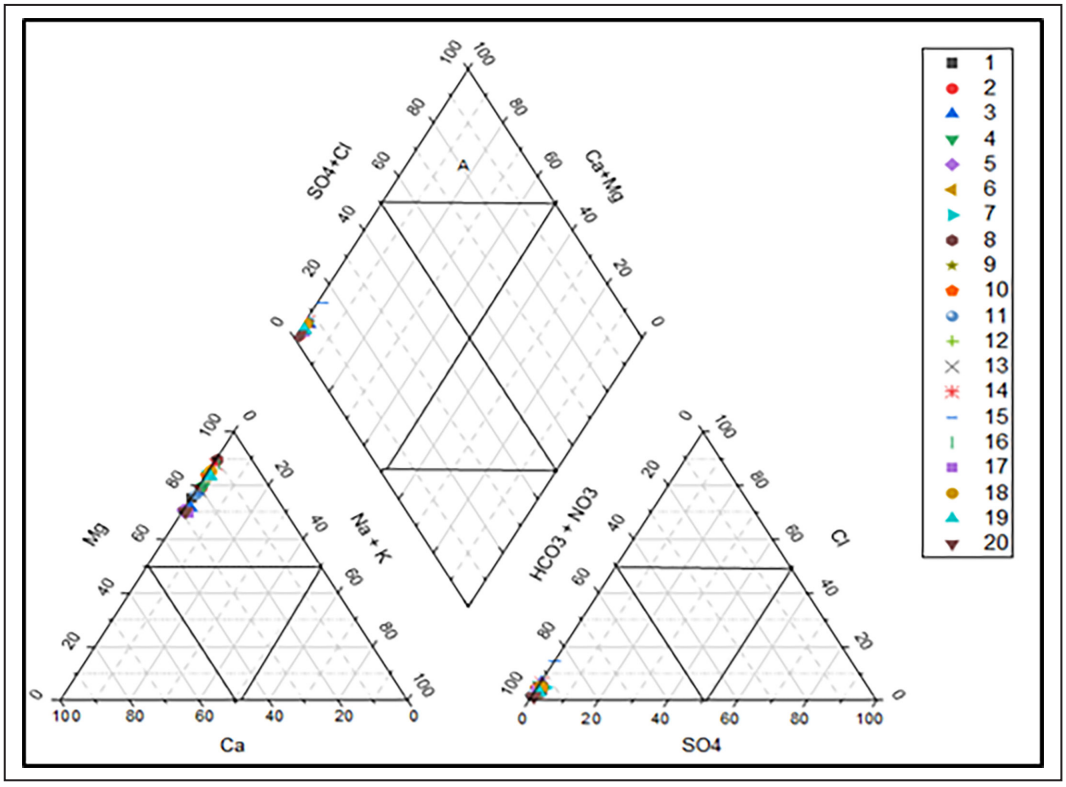

Figure 6: Piper diagram plotted using the Piper trilinear plot indicating hydrochemical facies of the samples under study.

shallow aquifers). It is simple to compute from routine lab measurements (pH, alkalinity, calcium, TDS/temperature),

Some limitations: some of the understudy samples where carbonate interaction dominates corrosion/scaling, it is observed seawater intrusion raises Na^+/Cl^- and sulfate, thereby increases ionic strength. This allows corrosion mechanisms to shift from carbonate-film control to chloride-induced pitting and general ionic-strength-driven corrosion resulted to corrosivity underestimation. Also, high salinity from seawater intrusion increases ionic strength and makes activity corrections important. LSI doesn't capture non-carbonate aggressors (dissolved oxygen, CO_2 partial pressure changes, chloride pitting), that are known drivers in coastal aquifers

The Ryznar Stability Index (RSI) addresses the corrosion risk of soil samples. It was observed that 88% of samples have values RSI >7 indicating severe corrosion risk, particularly in T3 and T15 where chloride exceeds 30 mg/L. The strong correlation (R^2=0.76) between RSI and chloride concentration supports the chloride-induced corrosion mechanism described by Roberge (2007).

Strengths. Based on this study, RSI often correlates better with observed corrosivity in distribution systems for waters that are undersaturated with respect to $CaCO_3$ hence the useful in preliminary screening of groundwater that may attack metal infrastructure. Also, it is simple to compute from the same field/lab data (pH, alkalinity, Ca^{2+}, T), and good for rapid assessments in large sample sets.

Limitations: RSI's calibration and thresholds were developed historically for certain temperate waters and may not translate directly where chloride-driven corrosion dominates. but relevant where seawater mixing, evaporites, and organic inputs occur. In shallow coastal aquifers where CO_2 degassing, pressure changes and temperature vary. RSI can be misrepresenting unless field protocols are tight.

Aggressiveness index of the groundwater samples under study range from 6.345 to 9.317 with a mean value of 8.045. This indicates the sample has 100% corrosion potential, 0% encrustation potential, and 0% neutral potential. As a result of the high concentration of degrading components in the water, the finding suggests that the borehole pipes and well of the research region are likely to be corrosive and hazardous to human health (Figure 7).

Strengths: AI uses pH, alkalinity and hardness parameters often available from routine sampling, making it attractive for rapid screening across many wells in the basin. AI can approximate the protective effect of $CaCO_3$ film without detailed equilibrium calculations and handy when lab resources are limited.

Limitations: Inconsistency in calculation methods can produce different classifications unless a single standard method is used. Insensitive to chloride/sulfate-driven pitting and to redox/biological factors, both relevant in coastal aquifers. AI can therefore miss major drivers of infrastructure corrosion in eastern Dahomey Basin coastal zones.

The Larson-Skold Index (LS) revealed 38% of samples under study to be greater than 1.2; this indicates a high chloride-sulfate corrosion, particularly in wells less than 30m depth. The remaining 62% with LS < 0.8 show stable $Fe(OH)_3$ films, consistent with observations by Larson and Skold (1958) in iron-rich aquifers.

Strengths: It is directly sensitive to halide (Cl^-) and sulfate loading; this is a major advantage in coastal aquifers in eastern Dahomey Basin where seawater intrusion elevates Cl^- and SO_4^{2-}. LS can therefore pick up chloride-

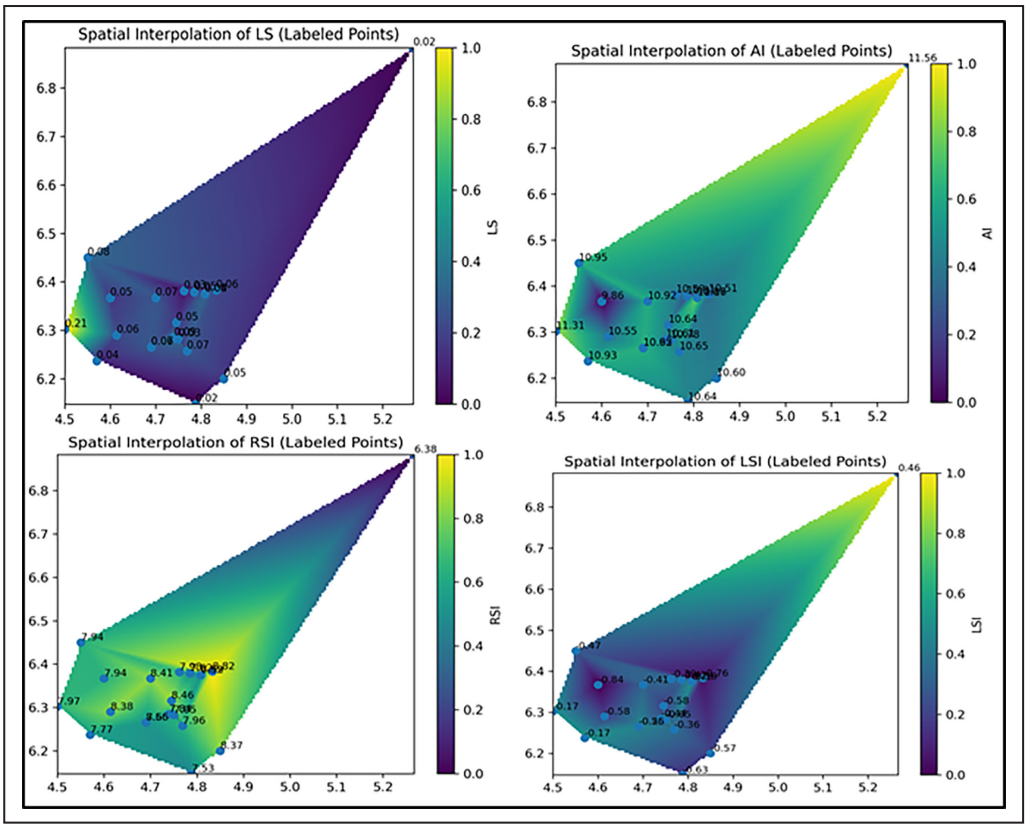

Figure 7: Spatial distribution of (A) Langelier Saturation Index (LSI), (B) Aggressive index, (C) Ryznar Stability Index (RSI) and (D) Larson–Skold Index values across the study area. The IDW approach applies a distance-decay weighting, ensuring that nearby water samples exert greater influence on interpolated values, which aligns with the localized nature of groundwater quality variation in the study area.

driven aggressiveness that carbonate-based indices miss. Multiple Dahomey Basin studies report elevated chloride/TDS near the coast, making LS highly relevant. This Predicts localized pitting and acid-type attack risk better than LSI in waters with high halide content (seawater-impacted).

Limitations: The Larson–Skold empirical relationships were calibrated on Great Lakes waters and steel pipes; extrapolation to other materials (concrete, copper, modern alloys) or to eastern Dahomey Basin's specific conditions requires caution. This doesn't include pH, DO, temperature in its action. These factors strongly affect corrosion rates. LS alone may fail to predict actual field corrosion without those data.

5.2.2 Spatial Distribution of Corrosion and Encrustation Potentials

Spatial analysis revealed clear patterns in corrosion and encrustation potentials across the study area (Figure 7). Samples from coastal locations (within 5 km of coastline) showed significantly higher corrosion tendencies, attributed to seawater intrusion increasing ionic strength and chloride concentrations. The influence of tidal pumping on oxygen diffusion and mixing processes further enhances corrosion in these zones. Agricultural areas showed elevated nitrate concentrations (up to 12.3 mg/L) that can promote microbial corrosion through nutrient availability for corrosion-related bacteria. Industrial zones exhibited higher sulfate concentrations (up to 4.9 mg/L) and lower pH values (as low as 6.3), accelerating electrochemical corrosion processes (Revie and Uhlig 2008).

The spatial distribution of LSI values shows scaling tendencies predominant in inland areas where carbonate mineral dissolution increases calcium and bicarbonate concentrations, while corrosive tendencies dominate in coastal areas influenced by seawater intrusion (Figure 7).

Spatial interpolation of Corrosion and Encrustation Indices using Inverse Distance Weighting (IDW): In this study, Inverse Distance Weighting (IDW) was chosen for spatial interpolation of corrosion and encrustation indices (LSI, AI, LS) across the Eastern Dahomey Basin sampling points. IDW was preferred because the dataset consisted of 20 moderately clustered samples, insufficient for reliable variogram modeling required by geostatistical Kriging. Furthermore, corrosion indices are locally sensitive hydrochemical parameters, for which deterministic methods such as IDW provide more robust and interpretable spatial patterns.

5.3. Global Perspectives on Corrosion and Encrustation Studies

The hydrochemical behavior observed in this study shows strong consistency with earlier regional investigations while also highlighting important local variations. The classification of approximately 30% encrustation potential aligns closely with findings from the Niger Delta aquifer systems, where Amah et al. (2008) reported moderate to high encrustation tendencies largely controlled by iron-rich groundwater, reducing conditions, and microbial activity. In both cases, iron precipitation—rather than carbonate scaling—plays a dominant role, reflecting

similar sedimentary environments, organic matter abundance, and redox-sensitive geochemical processes typical of deltaic settings (Revie and Uhlig 2008). However, the corrosion potential identified in this study exceeds values reported for the Benin Formation by Offodile (2002). This discrepancy is plausibly attributed to elevated chloride concentrations, which significantly enhance water aggressiveness by increasing electrical conductivity and promoting electrochemical reactions on metal surfaces. Chloride-induced corrosion has been widely documented in coastal and near-coastal aquifers worldwide, where marine influence, saline intrusion, or evaporative concentration intensifies corrosive conditions compared to inland sedimentary basins.

Furthermore, the mechanism of encrustation in the present study differs fundamentally from carbonate-dominated systems described in northern Nigeria. Etu-Efeotor (1997) demonstrated that groundwater scaling in crystalline and semi-arid northern terrains is largely driven by calcium carbonate precipitation, controlled by high alkalinity, elevated pH, and temperature-induced degassing of CO_2. In contrast, the current study area exhibits iron-dominated encrustation, governed by redox fluctuations, iron oxidation, and microbial mediation rather than carbonate equilibrium. Similar iron-controlled scaling processes have also been reported in deltaic and alluvial aquifers in parts of Asia and South America, emphasizing the strong influence of depositional environment and groundwater chemistry on scaling mechanisms. Overall, these comparisons underscore that while the encrustation and corrosion indices observed in this study are regionally consistent with other Nigerian and global sedimentary aquifers, local geochemical conditions particularly chloride levels, redox state, and dominant mineral phases—play a decisive role in determining the severity and type of infrastructure deterioration in groundwater systems. Recent studies on coastal aquifer management have highlighted the increasing threat of seawater intrusion due to climate change and sea-level rise, which exacerbates corrosion problems in coastal infrastructure (Abd-Elaty et al. 2022). The findings of this study align with global observations that coastal groundwater systems are experiencing increasing corrosion risks due to changing hydrological conditions (Oyeyemi et al. 2023).

The iron encrustation mechanism differs from carbonate-dominated systems in northern Nigeria, reflecting the unique hydrogeochemical, environment of the coastal Dahomey Basin.

Yenagoa, Bayelsa; some Niger Delta sites show very low EC and TDS, often < 50–20 µS/cm and < 20 mg/L, reflecting freshwater environment. It is observed in Lagos, Saudi Arabia exhibit EC ranging from 1000 to 1200 µS/cm while TDS reveale up to 700 mg/L. this indicates they are moderately mineralised aquifers, reflecting dissolution and anthropogenic inputs. The coastal environment of Tanzania, specifically Kilwa Kisiwani exhibit very highly Saline and Mineralised Groundwater, indicating the water has very high EC (up to about 4600 µS/cm) with

TDS (>2500 mg/L), commonly due to coastal (Hussain et al. 2019) or evaporitic influences (Tables 12 and 13).

Table 12: The review of various corrosion and encrustation parameters their possible outcomes and implications.

Location	Parameters Measurement	Results	Implications
Dahomey: Benin coastal aquifer	Extent of seawater intrusion; hydrochemical facies; delineation of boundary zones of intrusion.	Areas like Dahomey show evidence of seawater intrusion; certain wells are contaminated. Salinity, chloride elevated beyond background.	Even moderate saline intrusion several km inland; demands monitoring & management.
Parts of Niger Delta, Nigeria	Saltwater intrusion in coastal island aquifers; depth to interface; hydrochemical ratios.	Depth to freshwater-saltwater interface as shallow as **10–15 m**, depending on tidal phase/elevation. Strong hydrochemical signals: elevated TDS, EC, salinity, Cl^-, Na^+, K^+.	Very shallow interface means wells are highly vulnerable; infrastructure in shallow wells likely exposed to corrosive/inhospitable water.
Eastern Saudi Arabia (multi-layered aquifers)	Effects of seawater intrusion on groundwater quality; suitability for human/agricultural use.	Documented elevated salinity, poor suitability in some zones; groundwater becomes "unsuitable" for some uses as intrusion increases. Exact thresholds vary, but values well exceeding safe drinking/irrigation limits in affected layers.	Coastal aquifers under strong stress from human use + hydrochemical shift; management and/or mitigation required.
Global / General Coastal Context	Rates / extent of intrusion; risk behavior; role of over-pumping and sea level rise.	>1% seawater mixing makes water non-potable by taste; sea level rise of ~10cm can move interface inland hundreds of meters (on shallow gradients) in some coastal plains. In Spain: ~58% of the 82 coastal hydrogeological units show some seawater intrusion.	Coastal aquifers worldwide are already impacted; even small degrees of intrusion shift hydrochemistry enough to affect usability, corrosion, etc.

Table 13: Global perspectives of physicochemical parameters with data from the study area.

Location	EC Range (µS/cm)	TDS mg/L	Salinity (PSU)	pH	(Cl^-) mg/L
Study Area	1424.7	684.8	**0.4**	**7.0**	16.6
Niger Delta	19–24	9–183	0.17		
Bayelsa	6.23–13.74	5.77–18.30			
Lagos	450–1190	247.5–589.7			
Saudi Arabia	382–1214	258–775		6.65–8.26	19–202
Gombe	193.9–350	198–345			
Tanzania	1160–4620	754–3003			

6. Conclusion

This study provides comprehensive evidence that groundwater in the Eastern Dahomey Basin presents dual threats of corrosion and encrustation, with significant spatial variability correlated with coastal proximity and land use patterns. The hydrochemical analysis reveals that seawater intrusion, mineral dissolution, and anthropogenic activities collectively influence corrosion and encrustation processes. The application of multiple indices provides a robust assessment of these threats and offers insights for sustainable water resource management in coastal regions. The findings indicate that infrastructure development in the region must account for these hydrochemical challenges to ensure long-term sustainability and water security. The integration of geospatial analysis with hydrochemical assessment provides a valuable approach for targeted management interventions.

Based on the findings from the study area, it is recommended that the use of corrosion-resistant materials such as 316L stainless steel or high-density polyethylene (HDPE) for casing and pipelines in high-corrosion zones identified through spatial mapping. This can be complemented with introducing cathodic protection systems for existing mild steel infrastructure. Adopting periodic (6-month interval) descaling with citric acid for affected boreholes, coupled with calcite contactors installation to raise pH and LSI values in corrosive waters in order to reduce corrosion potential while maintaining water quality. Other recommendations include, establishing quarterly monitoring of LSI, RSI, and chloride concentrations in high-risk areas. Conduct annual video inspection of well casings to assess corrosion and encrustation damage. Enforce setback distances of at least 500 meters for new boreholes near the coastline to minimize seawater intrusion impacts. Develop integrated coastal zone management plans that address groundwater extraction rates and land use practices affecting aquifer vulnerability. It is also proposed to conduct a long-term monitoring program to assess seasonal variations in corrosion and encrustation potentials. Investigating the effectiveness of various mitigation measures under local conditions will assist to combact the manance of corrosion-encrustation challenges. Above all, it is required to explore the potential of novel materials and coatings for improved corrosion resistance.

Acknowledgements

This research was supported by the Department of Mineral and Petroleum Resources Engineering Technology, The Federal Polytechnic, Ado Ekiti. The authors acknowledge the technical support provided by the Keys Laboratory of Cenozoic Geology and Environment, Institute of Geology and Geophysics, CAS, China. We also thank community members and local authorities for their assistance during field sampling.

Author's disclaimer

Funding

No specific funding was received for this study.

Informed Consent

Not applicable.

Ethical Approval

Not applicable.

Conflict of Interest

The author declares no conflict of interest.

Data Availability

All data generated or analyzed during this study are included in this published article.

Authorship credits

Author	A	B	C	D	E	F
ROF						

A - Study design/ Conceptualization **B** - Investigation/ Data acquisition
C - Data Interpretation/ Validation **D** - Writing
E - Review/Editing **F** - Supervision/Project administration

References

Abd-Elaty I., Kushwaha N.L., Grismer M.E., Elbeltagi A., Kuriqi A. 2022. Cost-effective management measures for coastal aquifers affected by saltwater intrusion and climate change. Science of the Total Environment, 836, 155656. https://doi.org/10.1016/j.scitotenv.2022.155656

Acharya S., Sharma S.K., Khandegar V. 2019. Assessment and hydro-geochemical characterization for groundwater quality and corrosion-scaling potential. Data in Brief, 18, 928-938. https://doi.org/10.1016/j.dib.2018.03.120

Adelekan B.A, Abegunde K.D. 2011. Heavy metals contamination of soils and groundwater in auto-mechanic villages: case studies from Ibadan, Nigeria. International Journal of Physical Science, 6(5), 1045-1058. https://doi.org/10.5897/IJPS10.495

Aladejana J.A.; Kalin R.M.; Sentenac P.; Hassan I. 2021. Groundwater quality index as a hydrochemical tool for monitoring saltwater intrusion into coastal freshwater aquifer of Eastern Dahomey Basin, Southwestern Nigeria. Groundwater for Sustainable Development, 13, https://doi.org/10.1016/j.gsd.2021.100568

Amah E.A, Esu E.O., Ntekum E.E.U. 2008. Evaluation of corrosion encrustation potential of groundwater wells in Calabar. Global Journal of Geological Sciences, 6(1), 1-8 https://doi.org/10.4314/gjgs.v6i1.18748

Appelo C.A.J., Postma D. 2004. Geochemistry, groundwater and pollution. 2nd ed. CRC Press. https://doi.org/10.1201/9781439833544

Barlow P.M. 2003. Ground water in freshwater-saltwater environments of the Atlantic Coast. USGS Circular 1262. Reston, Virginia, U.S. Geological Survey. Available on line at: https://pubs.usgs.gov/circ/2003/circ1262/pdf/circ1262.pdf / (accessed on 2 February 2026)

Etu-Efeotor J.O. 1997. Fundamentals of petroleum geology. (An imprint of Jeson Services) Publisher Paragraphics, Port Harcourt, 146, 62- 64.

Fakolade O.R., Ikhane P.R., Hao Q., Ajibade O., Olusegun O., Olalekan O. 2024. REE Signatures in Quaternary Deposits: Implication for Provenance and Economic Potentials. https://doi.org/10.21203/rs.3.rs-3967339/v1

Fakolade O.R., Obasi R.A. 2012. The geochemical assessment of subsurface coastal plain clastic deposits of Eastern Dahomey Basin around Lagos area, South West Nigeria. International Journal of Science and Technology, 1(11), 300–307.

Freeze R. A., Cherry J.A. 1979. Groundwater. Science. Prentice-Hall, 604p. Available on line at: https://books.google.com.ng/books?id=8P7kFowKnGUC / (accessed on 7 February 2026)

Garg S.K. 2005. Hydrology and water resources engineering. 13rd ed. Delhi, Khanna Publishers.

Hussain M.S., Abd-Elhamid H.F., Javadi A.A., Sherif M.M. 2019. Management of Seawater Intrusion in Coastal Aquifers: A Review. Water, 11(12), 2467. https://doi.org/10.3390/w11122467

Ikhane P. R., Akintola A. I., Bankole S. I., Oyebolu O. O., Ogunlana E. O. 2013. Granulometric analysis and heavy mineralstudies of the sandstone facies exposed near Igbile, southwestern Nigeria. International Research Journal of Geology andMining (IRJGM),

3(4), 158-178. Available on line at: https://www.interesjournals.org/articles/Granulometric-analysis-and-heavy-mineral-studies-of-the-sandstone-facies-exposed-near-igbile-southwestern-nigeria.pdf/ (accessed on 7 February 2026).

Johnson E.E. 1975. Groundwater and wells: A reference book for the water-well. UOP Inc. 440 p.

Kingston D.R., Dishroon C.P., Williams P.A. 1983. Global basin classification system. American Association of Petroleum Geologists Bulletin, 67(12), 2175-2193. https://doi.org/10.1306/AD460936-16F7-11D7-8645000102C1865D

Langelier W. F. 1936. The analytical control of anti-corrosion water treatment. Journal AWWA, 28(10), v-vi, 1449-1668. https://doi.org/10.1002/j.1551-8833.1936.tb13785.x

Laniyan A.B, Ogunyinka, O.O, William, O.D., Okon, U.E. 2024. Assessment of underground water quality in some selected locations in Ewekoro local government, Ogun state, Nigeria. Journal of Management, Applied Sciences and Technology (JOMAT), 3(1). Available on line at: https://res.cloudinary.com/dzhohkjsb/image/upload/v1747648687/manuscript_uploads/1747648686292-Volume3-Number1-Article19%20%281%29.pdf.pdf/ (accessed on 7 February 2026).

Larson T.E., Skold R.V. 1958. Corrosion and tuberculation of cast iron. Journal American Water Works Association, 50(11), 1429–1432.

Madukwe H.Y., Obasi R.A., Fakolade O.R., Bassey C.E. 2015. Provenance, tectonic settings and source area weathering of the coastal plain sediments south west Nigeria. Scientific Research Journal, 3(2), 2201-2796. Available on line at: https://www.scirj.org/papers-0215/scirj-P0215235.pdf / (accessed on 7 February 2026)

McGarvey F.J., Smedley P.L., Beisly J., MacDonald A.M., Brown S.D.J. 2008. Corrosion and encrustation in groundwater boreholes. British Geological Survey Commissioned Report, CR/08/041.

National Population Commission (NPC). 2010. 2006 Population and Housing Census: Priority Table, Volume III – Population Distribution by Sex, State, LGA & Senatorial District. Abuja: National Population Commission. Available on line at: https://catalog.ihsn.org//catalog/3340/download/48521 / (accessed on 7 February 2026)

Nigeria Meteorological Agency (NiMet). 2018. Released Rainfall Data for Academic Research, Headquarters, Abuja Nigeria.

Obiefuna G., Orazulike D. 2011. Evaluation of corrosion and encrustation potentials of boreholes in yola area, Northeastern Nigeria. Trends in Applied Sciences Research. 6(10), 1197-1205. DOI: 10.3923/tasr.2011.1197.1205.

Offodile M.E. 2002. Groundwater study and development in Nigeria. 2nd ed. Mecon Press.

Ogunrayi O.A.; Mattah P.A.D.; Folorunsho R.; Jolaiya E.; Ikuomola O.J. 2024. A Spatio-temporal analysis of shoreline changes in the Ilaje coastal area of Ondo State, Nigeria, Journal of Marine Science and Engineering, 12, 18. https://doi.org/10.3390/jmse12010018

Ogunremi J., Oluwafemi O., Olaoye J. 2018. Assessment of the sustainable practices by artisanal fishers' association in Ilaje Local government area of Ondo State, Nigeria. International Journal of Development and Sustainability, 7(4), 1441-1448. Available on line at: https://isdsnet.com/ijds-v7n4-14.pdf / (accessed on 7 February 2026)

Olabode S., Mohammed M. 2016. Depositional facies and sequence stratigraphic study in parts of benin (Dahomey) basin SW Nigeria: implications on the re-interpretation of tertiary sedimentary successions. International Journal of Geosciences, 7, 210-228. http://dx.doi.org/10.4236/ijg.2016.72017

Olofinlade W.S., Daramola S.O., Olabode O.F. 2018. Hydrochemical and statistical modeling of groundwater quality in two constrasting geological terrains of southwestern Nigeria. Modeling Earth Systems and Environment, 4, 1405–1421. https://doi.org/10.1007/s40808-018-0486-1

Omaka F.I., Nwabue E.J.I., Igwe D.I. 2014. Physicochemical parameters and nutrients variations of streams and rivers In Abakaliki, Ebonyi State, Nigeria. Global NEST Journal, 16(1):114-123. https://doi.org/10.30955/gnj.000997

Oyeyemi K.D., Aizebeokhai A.P., Olaojo A.A., Okon, E. 2023. Hydrogeophysical investigation in parts of the Eastern Dahomey Basin, Southwestern Nigeria: Implications for sustainable groundwater resources development and management. Water, 15(16), 2862. https://doi.org/10.3390/w15162862

Puckorius P.R, Brooke J.M. 1991. A new practical index for calcium carbonate scale prediction in cooling tower Systems. Corrosion, 47, 280-284. https://doi.org/10.5006/1.3585256

Revie R.W., Uhlig H.H. 2008. Corrosion and corrosion control: An introduction to corrosion science and engineering. Hoboken, NJ, John Wiley & Sons. 513 p. https://doi.org/10.1002/9780470277270

Roberge P.R. 2007. Corrosion inspection and monitoring. Hoboken, NJ, John Wiley & Sons. https://doi.org/10.1002/0470099763

Ryznar J.W. 1944. A New index for determining the amount of calcium carbonate scale formed by water. Journal of American Water Works Association, 36, 472-483. https://doi.org/10.1002/j.1551-8833.1944.tb20016.x

Stumm W., Morgan J.J. 1996. Aquatic chemistry, chemical equilibria and rates in natural waters. 3rd Edition. New York, John Wiley & Sons, Inc.

Trethewey K.R., Chamberlain J. 1995. Corrosion for science and Engineering. 2nd Edition, England, Longman Group Limited.

Turner G., Morton A.C. 2007. The effects of burial diagenesis on detrital heavy mineral grain surface textures. In: Mange M.A., Wrigh, D.T. (eds.). Heavy minerals in use. Amsterdam; Boston, Elsevier, 2007. p. 393–412. (Developments in Sedimentology, 58).

Winston R.B. 2020. GW_Chart Version 1.30. [Computer software]. U.S. Geological Survey. https://doi.org/10.5066/P9Y29U1H

World Health Organization (WHO). 2017. Guidelines for drinking-water quality: fourth edition incorporating first addendum, 4th ed., 1st add. World Health Organization. Available on line at: https://iris.who.int/handle/10665/254637 / (accessed on 7 February 2026)

World Health Organization (WHO). 2006. Guidelines for drinking-water quality: incorporating first addendum. Vol. 1, Recommendations, 3rd ed. Available on line at: https://iris.who.int/handle/10665/43428 / (accessed on 7 February 2026)